Rare Met. (2020) 39(8):918–927
https://doi.org/10.1007/s12598-018-1063-5

RARE METALS
www.editorialmanager.com/rmet

Statistics of oxidation resistance of Ni–(0–15)Co–(8–15)Cr–(0–5)Mo–(0–10)W–(3–8)Al–(0–5)Ti–(0–10)Ta–0.1C–0.01B superalloys at 1000 °C by compositional variations

Si-Jun Park, Kyu-Hyuk Lee, Seong-Moon Seo, Hi-Won Jeong, Young-Soo Yoo, HeeJin Jang*

Received: 11 November 2017 / Revised: 10 January 2018 / Accepted: 20 April 2018 / Published online: 16 May 2018

Abstract The effects of alloying elements (Co, Cr, Mo, W, Al, Ti, and Ta) on the oxidation resistance of Ni–(0–15)Co–(8–15)Cr–(0–5)Mo–(0–10)W–(3–8)Al–(0–5)Ti–(0–10)Ta–0.1C–0.01B alloys were studied. The sample compositions were designed by the Box–Behnken method of design of experiments (DOE). The alloying elements show complicated effects on the mass gain due to oxidation, depending on the alloy composition. Al reduces the mass gain largely. The other elements except Al do not appear to exert a strong effect on the oxidation rate on average, but their influences are shown clearly in the alloys with a low Al content. Co, W, and Ta reduce the oxidation rate, while Cr, Mo, and Ti promote oxidation. Ta is the most effective element in reducing the oxidation rate of the alloy with a low Al concentration. It is confirmed that a continuous Al_2O_3 layer is essentially required for high oxidation resistance. The oxide scale of easily oxidized alloys has various oxides such as $NiCr_2O_4$, $NiAl_2O_4$, NiO, Cr_2O_3, $CrTaO_4$, and TiO_2.

S.-J. Park
Multi-Material Research Center, Gwangju-Jeonnam Division, Korea Automotive Technology Institute, Gwangju 62207, Republic of Korea

K.-H. Lee
Department of Advanced Materials Engineering, Chosun University, Gwangju 61452, Republic of Korea

S.-M. Seo, H.-W. Jeong, Y.-S. Yoo
High Temperature Materials Group, Korea Institute of Materials Science, Changwon 51508, Republic of Korea

H. Jang*
Department of Materials Science and Engineering, Chosun University, Gwangju 61452, Republic of Korea
e-mail: heejin@chosun.ac.kr

Keywords High temperature oxidation; Alloy composition; Ni-based superalloy; Oxidation resistance; Design of experiments

1 Introduction

Ni-based superalloys have importance in high temperature corrosion environments including power plant, aerospace industry, and chemical plant. Such environments demand excellent resistance of alloys to corrosion and oxidation, as well as mechanical properties such as creep resistance, at a temperature near or above 1000 °C.

Superalloys consist of various alloying elements to reach high performance under heavy thermal and mechanical load. Ni-based superalloys usually include Co, Cr, Mo, W, Al, Ti, Ta, and some rare earth metals such as Ce, Ru, Re, Y, and La [1–6]. The role of each element is under the interest of researchers as to design a better superalloy. Some alloying elements show very clear and easily notable effects on the oxidation resistance. As known generally, Al and Cr are representatives in improving the oxidation resistance by forming a protective oxide layer. Cr_2O_3 is highly effective in resisting oxidation under a temperature up to 871 °C [3]. At a higher temperature, Al_2O_3 is the most important compound to reduce oxidation rate. The continuous layer of Al_2O_3 provides high protection to oxidation [3, 7–12]. Mo is known to increase the oxidation rate because it forms volatile MoO_3 [13–17]. W, Ta, and Ti are reported to be harmful or beneficial to oxidation resistance depending on the alloy composition [2, 18–20]. The inconsistent behavior of these elements is thought to be related to changes in oxygen activity and continuity of Al_2O_3 layer.

The researches about the oxidation properties of the alloys commonly use a controlled series of alloy compositions. The effects of the limited number of elements are examined by comparative study in a small group of alloys. By this conventional scheme, the role of an element in the oxidation process can be recognized from the measurements of mass change and analyses on the oxide composition and morphologies. However, as shown from some examples mentioned above, the role of an element changes in relation to the other elements in the alloy and such a behavior is detected rarely by the conventional methodology. A high-dimensional series of alloy samples and suitable ways are required to analyze a large bunch or data to figure out the complicated behavior of various elements. Therefore, a statistical methodology to design alloy compositions for the experiments and to analyze the data is employed in this study. The design of experiments (DOE) can provide an efficient way to analyze the effects of alloying elements on the oxidation rate by a statistical methodology. It has been used successfully in examining the effects of compositional or process factors on the properties of a material [1, 21–25]. The number of experiments can be minimized and the results are processed to give quantitative information on the effectiveness of variables.

In this study, the effects of Co, Cr, Mo, W, Al, Ti, and Ta was examined on the oxidation resistance of Ni-based superalloys with composition of Ni–(0–15)Co–(8–15)Cr–(0–5)Mo–(0–10)W–(3–8)Al–(0–5)Ti–(0–10)Ta–0.1C–0.01B at 1000 °C. The sample composition was designed by DOE and the results were analyzed statistically to assess the effects of each element and interactions between them.

2 Experimental

The alloy composition was designed by the Box–Behnken method of response surface methodology (RSM) to minimize the number of experimental runs. The Box–Behnken method is highly efficient in the experiments with a lot of factors, i.e., independent variables, and the optimum response is not supposed to be found at the limit values of all factors. In this method, the levels of independent variables are assigned according to the three coded levels as − 1, 0, and +1. The codes represent the lower limit, the center, and the upper limit values of an independent variable, respectively. Figure 1 is a schematic diagram for the Box–Behnken design for three factors. The center point which has the coded value of 0 corresponds to the central value of the experimental range of the factor. Similarly, the edge points, defined as − 1 or +1 by coded value, correspond to the highest or the lowest value of the factors. A Box–Behnken design for three factors includes 13 experimental combinations of factors. The central point was repeated several times in the experiment usually to confirm a stable extrapolation around the central region.

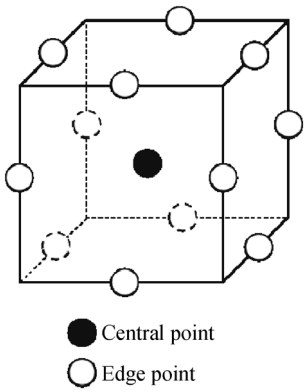

Fig. 1 Graphical representation of a Box–Behnken response surface design

The alloy composition is in the range of (0–15)Co–(8–15)Cr–(0–5)Mo–(0–10)W–(3–8)Al–(0–5)Ti–(0–10)Ta–0.1C–0.01B and the list of alloys designed for the test in this study are shown in Table 1. The alloys were made by vacuum arc melting and cut into coupons with 10 mm in diameter and 3 mm in height, and finished by 600 mesh SiC paper. Alumina crucibles of 20 mm × 20 mm × 15 mm were used to contain the specimens during oxidation tests, to measure the weight of the specimens including the scales fallen with cycling. The crucibles were pre-oxidized at 1000 °C for 1000 h to ensure no weight change during experiments.

Cyclic oxidation tests were performed as previously described [1]. The specimens were put in the box furnace at 400 °C and the temperature was increased up to 1000 °C at the rate of 5 °C·min^{-1}. After 15 h, the furnace was cooled down slowly by waiting for 2 h with the power off and then with the door open for about 2 h. The specimens were pulled out of the furnace when the temperature was 400 °C. The weight of each specimen was measured with its crucible after the temperature of the specimen reached room temperature of 20–25 °C as confirmed by an infrared thermometer. The changes in the total weight of the specimen and its crucible were recorded, assuming that the weight of the crucible was consistent during the oxidation tests. The phase, morphology, and composition of the oxide scales of the selected samples were analyzed by X-ray diffractometer (XRD, X'Pert PRO MPD), scanning electron microscope (SEM, Hitachi FE SEM S-4800) equipped with energy dispersive spectroscopy (EDS) after 20 cycles of oxidation tests.

The mass gain after oxidation was statistically analyzed as a response surface model. The mass gain, i.e., response,

Table 1 List of alloy compositions used in this study (wt%)

Alloys	Co	Cr	Mo	W	Al	Ti	Ta	C	B	Ni
RSM-1	7.5	11.5	2.5	0	3.0	0	5	0.1	0.01	Bal.
RSM-2	7.5	11.5	2.5	10	8.0	0	5	0.1	0.01	Bal.
RSM-3	7.5	11.5	2.5	10	3.0	5.0	5	0.1	0.01	Bal.
RSM-4	7.5	11.5	2.5	0	8.0	5.0	5	0.1	0.01	Bal.
RSM-5	0	11.5	2.5	5	5.5	0	0	0.1	0.01	Bal.
RSM-6	15.0	11.5	2.5	5	5.5	5.0	0	0.1	0.01	Bal.
RSM-7	15.0	11.5	2.5	5	5.5	0	10	0.1	0.01	Bal.
RSM-8	0	11.5	2.5	5	5.5	5.0	10	0.1	0.01	Bal.
RSM-9	7.5	8.0	2.5	5	3.0	2.5	0	0.1	0.01	Bal.
RSM-10	7.5	15.0	2.5	5	8.0	2.5	0	0.1	0.01	Bal.
RSM-11	7.5	15.0	2.5	5	3.0	2.5	10	0.1	0.01	Bal.
RSM-12	7.5	8.0	2.5	5	8.0	2.5	10	0.1	0.01	Bal.
RSM-13	0	8.0	2.5	0	5.5	2.5	5	0.1	0.01	Bal.
RSM-14	15.0	15.0	2.5	0	5.5	2.5	5	0.1	0.01	Bal.
RSM-15	15.0	8.0	2.5	10	5.5	2.5	5	0.1	0.01	Bal.
RSM-16	0	15.0	2.5	10	5.5	2.5	5	0.1	0.01	Bal.
RSM-17	7.5	11.5	0	0	5.5	2.5	0	0.1	0.01	Bal.
RSM-18	7.5	11.5	5.0	10	5.5	2.5	0	0.1	0.01	Bal.
RSM-19	7.5	11.5	5.0	0	5.5	2.5	10	0.1	0.01	Bal.
RSM-20	7.5	11.5	0	10	5.5	2.5	10	0.1	0.01	Bal.
RSM-21	0	11.5	0	5	3.0	2.5	5	0.1	0.01	Bal.
RSM-22	15.0	11.5	5.0	5	3.0	2.5	5	0.1	0.01	Bal.
RSM-23	15.0	11.5	0	5	8.0	2.5	5	0.1	0.01	Bal.
RSM-24	0	11.5	5.0	5	8.0	2.5	5	0.1	0.01	Bal.
RSM-25	7.5	8.0	0	5	5.5	0	5	0.1	0.01	Bal.
RSM-26	7.5	15.0	5.0	5	5.5	0	5	0.1	0.01	Bal.
RSM-27	7.5	15.0	0	5	5.5	5.0	5	0.1	0.01	Bal.
RSM-28	7.5	8.0	5.0	5	5.5	5.0	5	0.1	0.01	Bal.
RSM-29	7.5	11.5	2.5	5	5.5	2.5	5	0.1	0.01	Bal.
RSM-30	7.5	11.5	2.5	5	5.5	2.5	5	0.1	0.01	Bal.
RSM-31	7.5	11.5	2.5	5	5.5	2.5	5	0.1	0.01	Bal.
RSM-32	7.5	11.5	2.5	10	3.0	0	5	0.1	0.01	Bal.
RSM-33	7.5	11.5	2.5	0	8.0	0	5	0.1	0.01	Bal.
RSM-34	7.5	11.5	2.5	0	3.0	5.0	5	0.1	0.01	Bal.
RSM-35	7.5	11.5	2.5	10	8.0	5.0	5	0.1	0.01	Bal.
RSM-36	15.0	11.5	2.5	5	5.5	0	0	0.1	0.01	Bal.
RSM-37	0	11.5	2.5	5	5.5	5.0	0	0.1	0.01	Bal.
RSM-38	0	11.5	2.5	5	5.5	0	10	0.1	0.01	Bal.
RSM-39	15.0	11.5	2.5	5	5.5	5.0	10	0.1	0.01	Bal.
RSM-40	7.5	15.0	2.5	5	3.0	2.5	0	0.1	0.01	Bal.
RSM-41	7.5	8.0	2.5	5	8.0	2.5	0	0.1	0.01	Bal.
RSM-42	7.5	8.0	2.5	5	3.0	2.5	10	0.1	0.01	Bal.
RSM-43	7.5	15.0	2.5	5	8.0	2.5	10	0.1	0.01	Bal.
RSM-44	15.0	8.0	2.5	0	5.5	2.5	5	0.1	0.01	Bal.
RSM-45	0	15.0	2.5	0	5.5	2.5	5	0.1	0.01	Bal.
RSM-46	0	8.0	2.5	10	5.5	2.5	5	0.1	0.01	Bal.
RSM-47	15.0	15.0	2.5	10	5.5	2.5	5	0.1	0.01	Bal.
RSM-48	7.5	11.5	5.0	0	5.5	2.5	0	0.1	0.01	Bal.
RSM-49	7.5	11.5	0	10	5.5	2.5	0	0.1	0.01	Bal.
RSM-50	7.5	11.5	0	0	5.5	2.5	10	0.1	0.01	Bal.
RSM-51	7.5	11.5	5.0	10	5.5	2.5	10	0.1	0.01	Bal.
RSM-52	15.0	11.5	0	5	3.0	2.5	5	0.1	0.01	Bal.
RSM-53	0	11.5	5.0	5	3.0	2.5	5	0.1	0.01	Bal.
RSM-54	0	11.5	0	5	8.0	2.5	5	0.1	0.01	Bal.
RSM-55	15.0	11.5	5.0	5	8.0	2.5	5	0.1	0.01	Bal.
RSM-56	7.5	15.0	0	5	5.5	0	5	0.1	0.01	Bal.
RSM-57	7.5	8.0	5.0	5	5.5	0	5	0.1	0.01	Bal.
RSM-58	7.5	8.0	0	5	5.5	5.0	5	0.1	0.01	Bal.
RSM-59	7.5	15.0	5.0	5	5.5	5.0	5	0.1	0.01	Bal.
RSM-60	7.5	11.5	2.5	5	5.5	2.5	5	0.1	0.01	Bal.
RSM-61	7.5	11.5	2.5	5	5.5	2.5	5	0.1	0.01	Bal.
RSM-62	7.5	11.5	2.5	5	5.5	2.5	5	0.1	0.01	Bal.

is expressed as a function of the content of the seven alloying elements as in the following equation:

$$y = \beta_0 + \sum_{i=1}^{i=7} \beta_i x_i + \sum_{i=1}^{i=7} \beta_{ii} x_i^2 + \sum_{i=1}^{i=7} \sum_{i=1}^{i=7} \beta_{ij} x_i x_j, \quad (1)$$

where β_0 is the response at the center of the experiment, β_i is is the coefficient of main effects, β_{ii} is the coefficient of quadratic effects, and β_{ij} is the coefficient of linear by linear interaction effect. The coefficients were calculated by a regression analysis with the least squares method. x_i is the level of a factor, that is, the content of an alloying element in this study.

3 Results and discussion

The mass gain during oxidation tests is shown in Fig. 2 as a function of cycle number. The mass increases with oxidation, and the increasing rate is different for each alloy. The oxidation rate is rapid initially and then reduces gradually, except for the particular case of RSM-9 of which the mass increases almost linearly.

The mass gains for 62 alloy compositions measured at the end of cyclic oxidation tests were statistically analyzed. If the regression model is valid, the residuals should be normally distributed and scattered randomly about zero without any dependence on the observation order. However, Fig. 3 shows that the residuals do not meet these criteria, but also the coefficient of determination (R^2) is very low as 20.2%. It means that the regression model

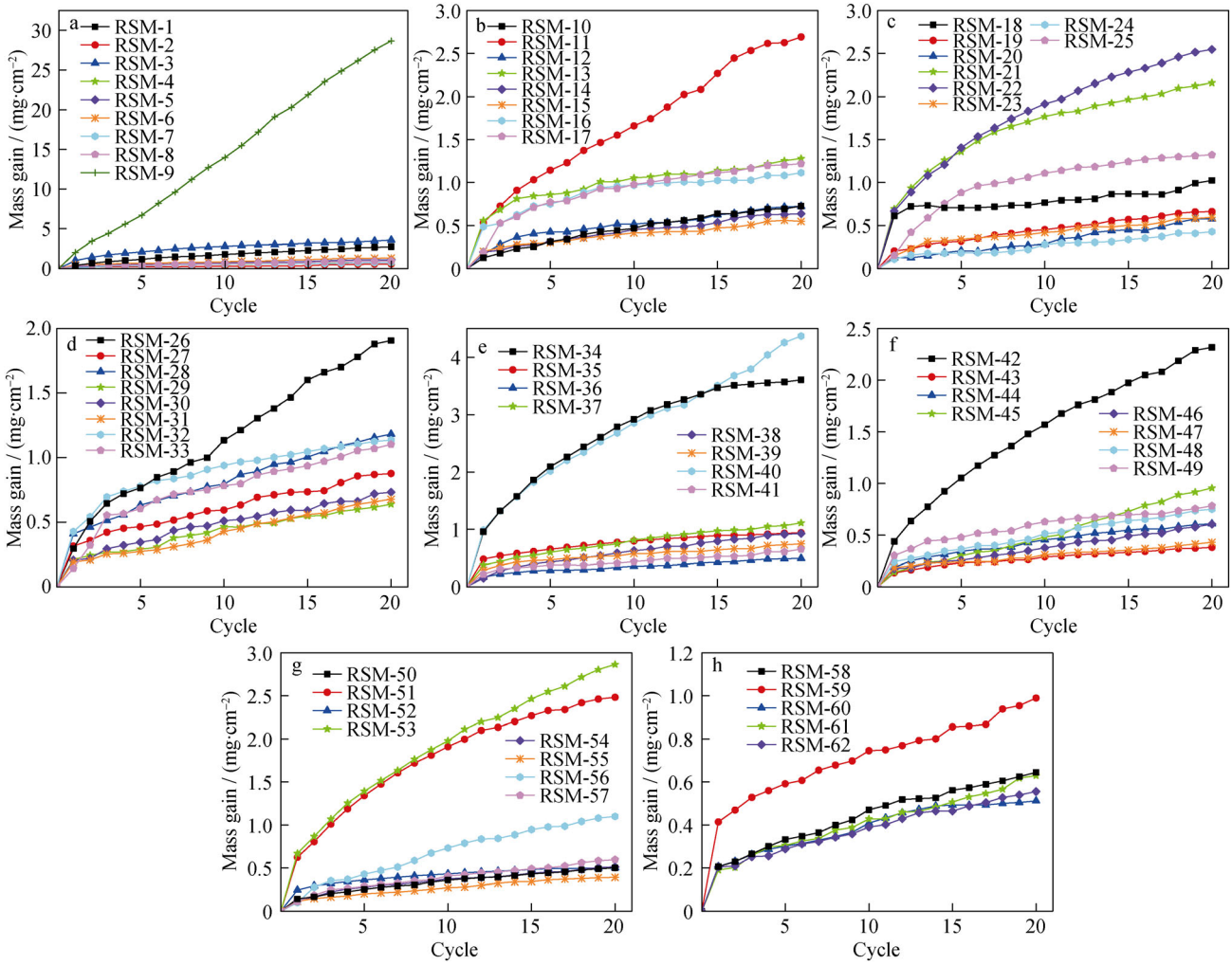

Fig. 2 Mass gain of Ni–(0–15)Co–(8–15)Cr–(0–5)Mo–(0–10)W–(3–8)Al–(0–5)Ti–(0–10)Ta–0.1C–0.01B alloys during cyclic oxidation at 1000 °C

practically fails to explain the experimental results. It is thought to originate in an outlier, that is, the mass gain of RSM-9 in this work. When an outlier influences the regression analysis, it is strongly recommended to exclude the outlier in the regression analysis [26].

Therefore, the regression analysis was performed excluding RSM-9. The residuals are normally and randomly distributed (Fig. 4) and the R^2 is as high as 89.1% for this case. The regression coefficient and the significance probability are shown in Table 2. The most influential element is Al. Al has a largely negative coefficient of − 0.95 and its calculated probability (P) is 0. It confirms that Al suppresses oxidation strongly, as generally known. Al * Al has also a P value of 0, but the coefficient is positive, meaning that the effect of Al reducing mass gain decreases with further increase in Al contents. Mo, Ti * Ti, Mo * Al, and Al * Ti terms, as well as Al and Al * Al, have P value less than 0.05. Mo is thought to increase the mass gain, judged from the positive coefficient. The positive coefficient of Ti * Ti implies that Ti promotes oxidative mass gain more in the alloy with higher Ti content. Mo * Al has also a positive coefficient, suggesting the possibility that high Mo content makes Al less effective in inhibiting oxidation or that high Al content facilitates more the effect of Mo which promotes oxidation. Al * Ti has negative coefficient and it suggests that Al and Ti have a synergistic effect in impeding oxidation, although Ti itself rarely affects the mass gain as shown from the low coefficient and the high P value of the Ti term.

Figure 5a depicts the main effect of each element on average. Co appears to reduce the mass gain a little, especially when the content is more than 7.5 wt%. Cr and Mo increase the mass gain slightly. W and Ta do not affect the mass gain. Al largely reduces the mass gain. The effect of Ti is very weak, but it seems to cause a small increase of mass gain with a higher content than 2.5 wt%. Figure 5b shows more detailed effects including interactions between alloying elements, which are not known from the main

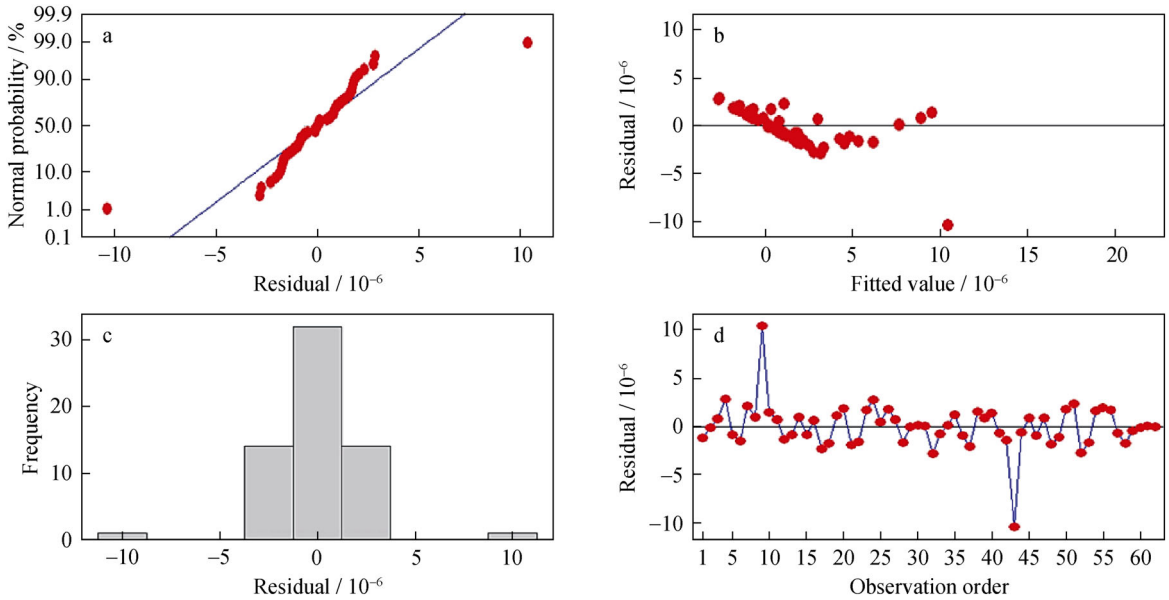

Fig. 3 Diagnostic plots: **a** normal probability plot of residuals, **b** residual versus fitted values, **c** histogram of residuals, and **d** residual versus order of data

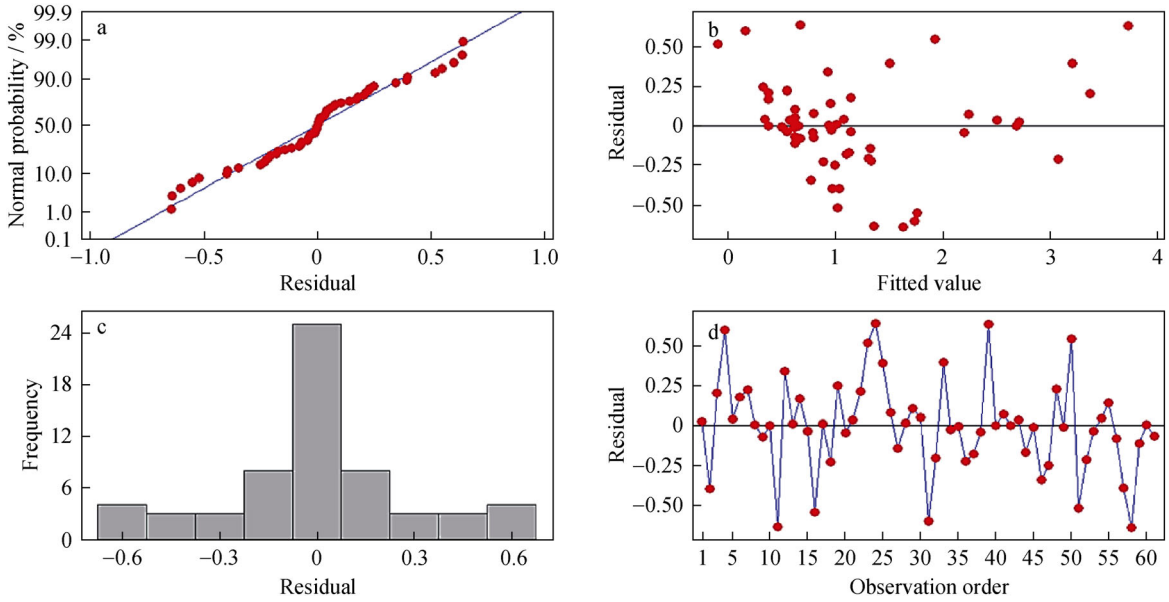

Fig. 4 Diagnostic plots excluding RSM-9: **a** normal probability plot of residuals, **b** residual versus fitted values, **c** histogram of residuals, and **d** residual versus order of data

effect plots (Fig. 5a). The main effect and interactions are described quantitatively by the coefficients shown in Table 2. Many of the terms have high *P* values. *P* value means significance probability and the terms with low *P* values than 0.05 are usually accepted to be meaningful with a high reliability. However, those with higher *P* values can have significance to some extent. The terms of Al and Mo have *P* values lower than 0.05, confirming that these elements certainly affect the oxidation, as known generally. Nevertheless, Table 2 shows that all the other elements appear to have statistically meaningful coefficients, as they have *P* values less than or around 0.05 for their linear or second-order terms.

It is revealed from the interaction plots of Co shown in the first column of Fig. 5b that the effect of Co on reducing the mass gain is significant only when Al concentration in the alloys is low (3.0 wt%). It means that Co is effective in protecting the alloy from oxidation, but Al is much stronger in forming protective layers.

Table 2 Results of regression analysis for mass gain after oxidation tests [S (standard error) = 0.4529, R^2 = 89.1%, R^2 (adjusted) = 73.9%]

Term	Coefficient	SE coefficient	T	P
Constant	0.624223	0.18491	3.376	0.002
Co	− 0.184700	0.09246	− 1.998	0.057
Cr	0.147129	0.09746	1.510	0.144
Mo	0.209621	0.09246	2.267	0.032
W	− 0.043510	0.09246	− 0.471	0.642
Al	− 0.953480	0.09746	− 9.784	0
Ti	0.121400	0.09246	1.313	0.201
Ta	− 0.083930	0.09746	− 0.861	0.397
Co * Co	− 0.163200	0.12423	− 1.314	0.201
Cr * Cr	0.161711	0.12707	1.273	0.215
Mo * Mo	0.023920	0.12423	0.193	0.849
W * W	0.149108	0.12423	1.200	0.241
Al * Al	0.764264	0.12707	6.015	0
Ti * Ti	0.267699	0.12423	2.155	0.041
Ta * Ta	0.202331	0.12707	1.592	0.124
Co * Cr	− 0.034410	0.16014	− 0.215	0.832
Co * Mo	0.152144	0.16014	0.950	0.351
Co * W	0.030901	0.16014	0.193	0.849
Co * Al	0.252609	0.16014	1.577	0.127
Co * Ti	0.099031	0.16014	0.618	0.542
Co * Ta	0.007989	0.16014	0.050	0.961
Cr * Mo	0.138389	0.16014	0.864	0.396
Cr * W	0.085474	0.16014	0.534	0.598
Cr * Al	− 0.356970	0.18491	− 1.931	0.065
Cr * Ti	− 0.131320	0.16014	− 0.820	0.420
Cr * Ta	− 0.280880	0.18491	− 1.519	0.141
Mo * W	0.307015	0.16014	1.917	0.067
Mo * Al	− 0.379460	0.16014	− 2.370	0.026
Mo * Ti	0.071239	0.16014	0.445	0.660
Mo * Ta	0.286708	0.16014	1.790	0.086
W * Al	0.159056	0.16014	0.993	0.330
W * Ti	0.285409	0.16014	1.782	0.087
W * Ta	0.257275	0.16014	1.607	0.121
Al * Ti	− 0.408560	0.16014	− 2.551	0.017
Al * Ta	0.155434	0.18491	0.841	0.409
Ti * Ta	− 0.103490	0.16014	− 0.646	0.524

Cr shows an interaction with Al and Ta. Cr–Al and Cr–Ta interaction plots from the second column of Fig. 5b show that the mass gain clearly depends on Cr only when the Al content is minimum (3.0 wt%) or Ta is not added in the alloy. Cr is well known to form a protective oxide film at relatively low temperature, but to form a volatile CrO_3 at a higher temperature such as 1000 °C [3, 7–12]. Cr may increase and decrease the mass along with different oxidation mechanisms. Formation of volatile CrO_3 results in a mass loss by itself, but volatilization can also accelerate mass gain by oxidation of other elements due to the low protectiveness of the oxide scale. The increasing mass gain of the low Al alloys with an increase in the Cr content is explained by this effect.

Mo also has a strong interaction with Al. The effect of Mo is highly noticeable in the alloys with a low Al content. It is thought to be related with volatilization of MoO_3 [13–17], which weakens the oxide scale. Mass loss by volatilization may be predominant in the early stage of oxidation, but prolonged oxidation and depletion of Mo will cause high oxidation rate of other elements. In addition, an interaction between Mo and W is observed. Mo generally causes a slight increase in the mass gain in the alloys with 5 wt%–10 wt% W, but reduces mass gain when its content is more than 2.5 wt% in the alloys without W.

W appears to be ineffective in the main effect plot (Fig. 5a), but the interaction plots (Fig. 5b) suggest that it has a different effect on the mass gain, depending on the concentration of other elements. The contradictory behavior of W results in the apparent ineffectiveness by average, as shown in Fig. 5a. W reduces the mass gain of the alloys with a low Al content as shown in the W–Al interaction plot. W has a high valance of 4+ or 6+ and hence it consumes more oxygen diffused into the scale than the other elements such as Al. W can contribute to retarding oxidation by capturing oxygen efficiently. This effect will be prominent when continuous Al_2O_3 layer cannot be formed due to low Al content. On the contrary, W slightly increases the mass gain of the alloys with high Mo content. W may retard formation and volatilization due to its low diffusion rate, thus suppressing the mass loss by volatilization. This presumption can be supported by a previous study, suggesting that W suppresses volatilization of Cr oxide from Ni–Cr–W alloys at a high temperature over 1100 °C [27].

Al generally causes a strong reduction of mass gain, but the degree of effectiveness varies by its interaction with other elements. Cr, Mo, and Ti enhance the effect of Al, while Co and Ta suppress it. This kind of interaction is noticeable when the Al content is less than 5.5 wt%. Actually, Al has the strongest interaction with itself, as proposed by the zero P value and coefficient of the Al * Al term (Table 2). The positive value of the coefficient (0.76) of Al * Al term implies that the high Al content attenuates the reducing effect of Al on the mass gain. Thus, the slope of the mass gain versus Al content plot decreases with an increase in Al content.

Ti has a strong effect on increasing the mass gain of the alloys with a low Al concentration. But this effect is highly suppressed by adding Al in high concentration of over

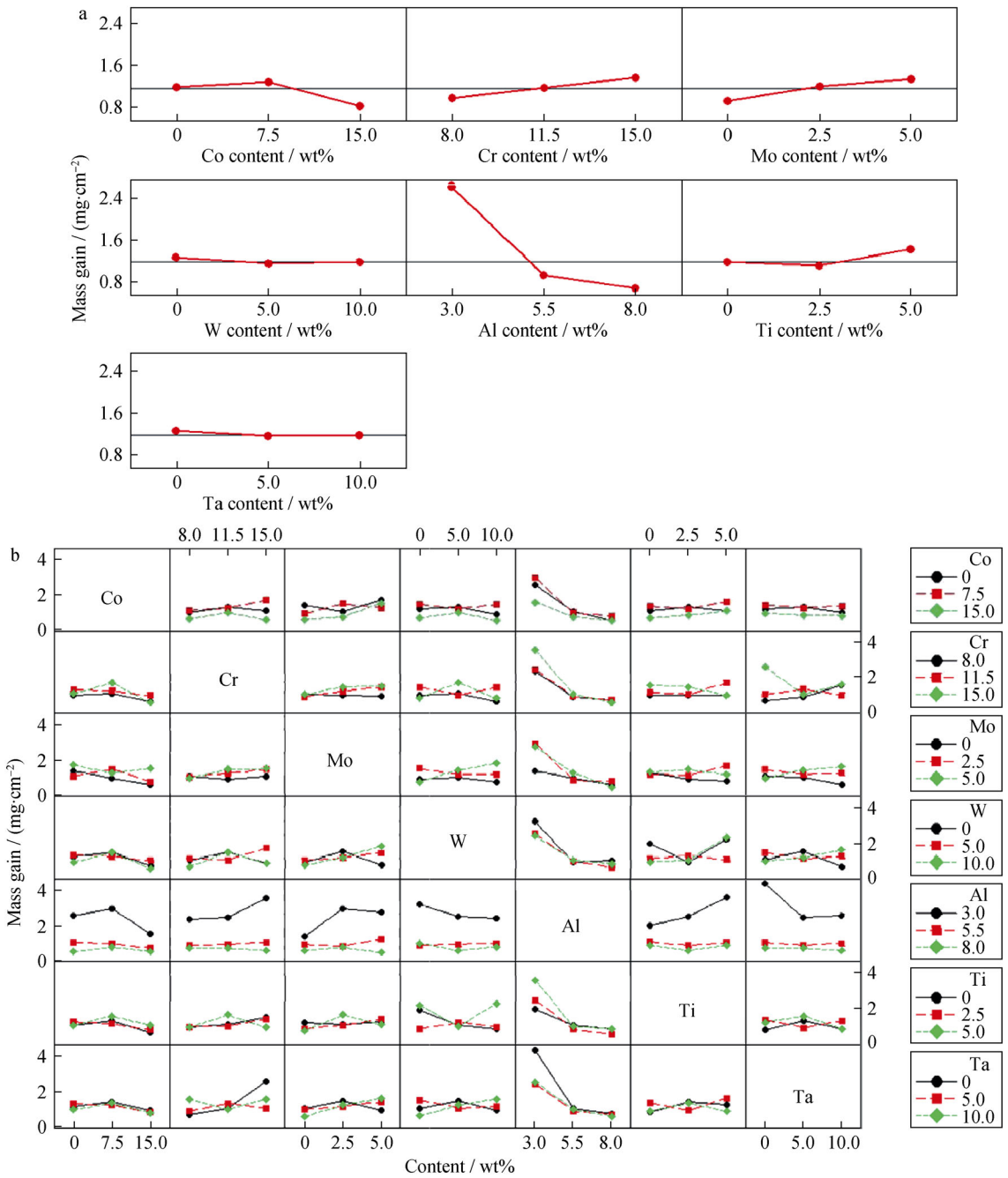

Fig. 5 **a** Main effects and **b** interactions of alloying elements on mass gain by oxidation at 1000 °C, as a statistical result excluding RSM-9

5.5 wt%. In an alloy with a low Al content, continuous Al layer is formed hardly because of low activity of Al. When Ti hinders the formation of a continuous Al oxide layer as in a previously reported case for a 5 wt% Al alloy at 850 °C [19], the oxidation resistance of the alloy will be weakened further by Ti. However, the same literature reported that Ti improves the oxidation resistance at 1000 °C because Ti reduces the concentration of oxygen vacancy in the Al_2O_3 layer. 5 wt% Al at 1000 °C is enough to form a continuous Al_2O_3 layer, while it is not at 850 °C [19]. Therefore, the effect of Ti on the mass gain is thought to depend on whether a continuous Al_2O_3 layer is formed or not, determined by thermally driven diffusion or by the concentration of Al.

Ta reduces the mass gain when Cr content is high (15 wt%) or Al content is low (3.0 wt%) (Fig. 5b). This effect is shown clearly when its concentration is less than 5 wt%. It is also noticed that Ta slightly increases the mass gain for the other alloys, especially with high Mo or W. Thus, the effect of Ta is not recognized when averaged

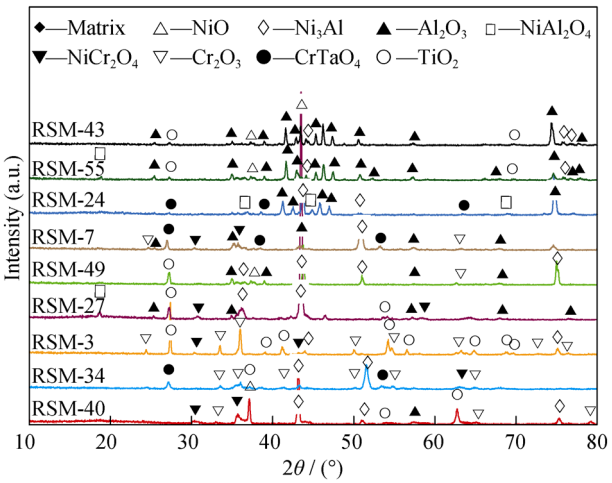

Fig. 6 XRD patterns of selected alloys after cyclic oxidation at 1000 °C

(Fig. 5a). Ta has very strong interaction with Al. The mass gain decreases significantly with an increase in the Ta content when the content of Al is 3 wt%, although Ta rarely affects the mass gain of the alloys with a high Al content. Park et al. [18] previously reported very similar result that Ta lowers the mass gain notably only in the alloy with a low Al content. Several researchers have proposed that a high concentration of Ta suppresses the formation of Al_2O_3 by lowering the oxygen activity because Ta has a higher valence than Al [28, 29] or by impeding Al diffusion due to its large size [30]. Low oxygen activity results in a discontinuity of Al_2O_3 in the alloy with a low Al content. In this situation, Ta has an important role in capturing oxygen and retarding oxidation. However, Al_2O_3 can form a continuous layer in the alloy with a high Al content, regardless of Ta content. In this case, the oxidation resistance of the alloy depends more on the Al_2O_3 layer than on Ta oxide.

XRD diffraction pattern (Fig. 6) shows that the oxide layer is composed of NiO and Al_2O_3. Relatively weak diffraction peaks for $NiAl_2O_4$, $NiCr_2O_4$, Cr_2O_3, $CrTaO_4$, and TiO_2 indicate that these oxides are formed in small fractions. SEM images in Fig. 7 show typical cross sections of oxidized alloys, which are categorized by the oxidation rate. All alloys have Al_2O_3 layer commonly just over the metallic phase. The alloys which are easily oxidized have a $NiCrO_4$ layer on the Al_2O_3 layer and NiO and Cr_2O_3 are formed partly (Fig. 7a–c). The alloys of mid-rate oxidation have $NiAl_2O_4$ or $NiCr_2O_4$, sometimes accompanying TiO_2 (Fig. 7d–f). The oxide scale of oxidation-resistive alloys has only Al_2O_3 layer, as shown in Fig. 7g–i. The intermetallic phases enriched with Cr, Co, Mo, and W are located just below the oxide layer of highly resistant alloys (Fig. 7g–i), but it seems that these alloying elements are a

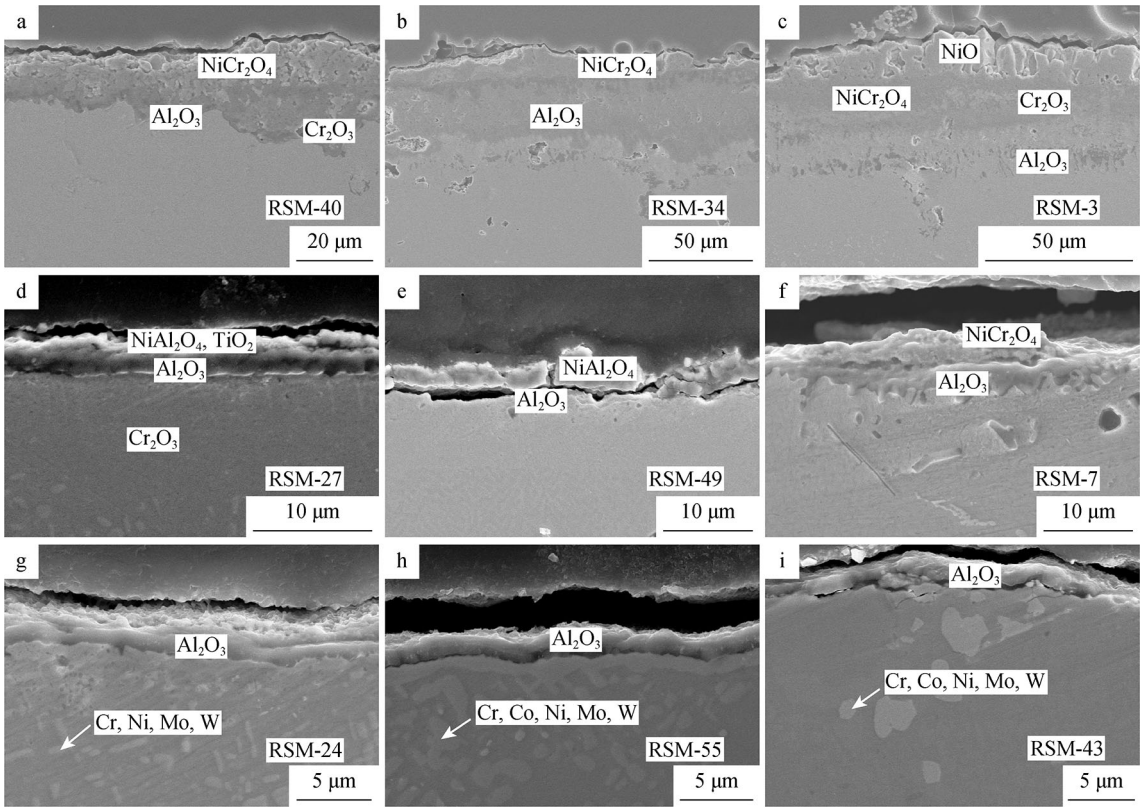

Fig. 7 SEM images of selected alloys with **a–c** high, **d–f** moderate, and **g–i** low oxidation rates after cyclic oxidation at 1000 °C

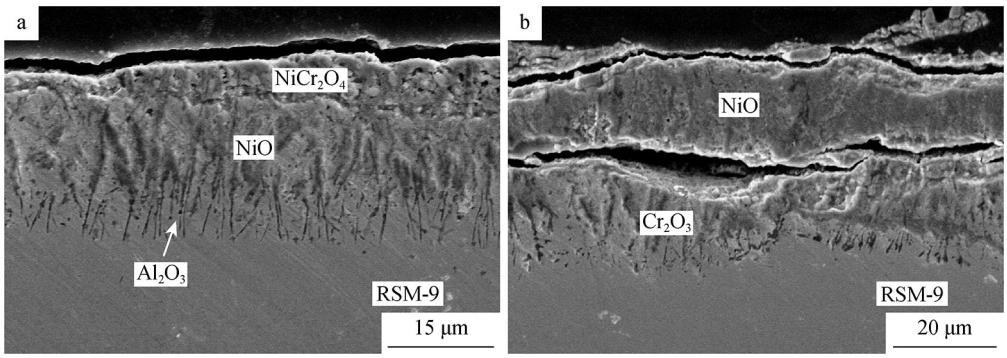

Fig. 8 SEM images of RSM-9 after oxidation at 1000 °C

little depleted at the vicinity of the oxide/alloy interface of the easily oxidized alloys (Fig. 7a–f). Depletion of intermetallic phase is thought to be related to the high outward diffusion rate of metallic ions in alloys with a high oxidation rate.

Figure 8 shows the cross-sectional image of RSM-9 which has exceptionally high oxidation rate (Fig. 2a). Al_2O_3 forms a needle-like shape instead of a continuous layer. NiO, Cr_2O_3, and $NiCr_2O_4$ are observed in the outer layer. NiO grows to be a thick layer in some areas and a crack is developed between oxide layers (Fig. 8b). It is widely known that a continuous Al_2O_3 layer is essentially required for Ni-based superalloys to be resistant to oxidation at a high temperature above 900 °C because Cr oxide is not so protective at this temperature [3, 10–12]. RSM-9 has a small Al content of 3 wt%, so a relatively low oxidation resistance is expected. In addition, RSM-9 does not contain Ta, which is the most effective element for low Al alloys to resist oxidation as suggested by the interaction plots shown in Fig. 5b. This alloy has the mid-level amount of other beneficial elements, i.e., Co and W, but they could not facilitate the formation of a continuous Al_2O_3 layer.

4 Conclusion

The effects of alloying elements (Co, Cr, Mo, W, Al, Ti, and Ta) on the oxidation resistance were examined at 1000 °C. 62 samples of Ni–(0–15)Co–(8–15)Cr–(0–5)Mo–(0–10)W–(3–8)Al–(0–5)Ti–(0–10)Ta–0.1C–0.01B were designed by the Box–Behnken method of DOE and the mass gain and oxide scale structure were examined. The main effects of each element and interactions between them were examined based on the mass gain after oxidation. The major findings are as follows.

Al largely reduces the oxidation rate. Reduction of mass gain by Al addition becomes less effective with an increase in Al content. Co has some effect on reducing mass gain by oxidation, especially for the alloys with low Al content of 3 wt%. Cr, Mo, and Ti slightly increase mass gain by oxidation on average. This effect is strong only for 3 wt% Al alloys. W and Ta appear to affect the oxidation rate slightly, as averaged for the whole group of samples. However, they clearly decrease the oxidation rate of the alloys with 3 wt% Al.

The composition and phases of the oxide scale of the selected samples suggest the followings. The alloy with high oxidation resistance has continuous Al_2O_3 scale without other complex oxides. For an alloy with low Al content, Ta is the most effective element to improve the protectiveness of the scale.

Acknowledgements This work was financially supported by the Fundamental R&D Program for Core Technology of Materials (No. 10041233) and the Human Resources Program in Energy Technology of the Korea Institute of Energy Technology Evaluation and Planning (KETEP) (No. 20174030201620).

References

[1] Park SJ, Seo SM, Yoo YS, Jeong HW, Jang HJ. Statistical study of the effects of the composition on the oxidation resistance of Ni-based superalloys. J Nanomater. 2015. https://doi.org/10.1155/2015/929546.
[2] Yun DW, Seo SM, Jeong HW, Yoo YS. Effect of refractory elements and Al on the high temperature oxidation of Ni-base superalloys and modelling of their oxidation resistance. J Alloy Compd. 2017;710(5):8.
[3] Donachie MJ, Donachie SJ. Superalloys: A Technical Guide, vol. 2. Ohio: ASM International Ltd; 2002. 1.
[4] Guo H, Li D, Zheng L, Gong S, Xu H. Effect of co-doping of two reactive elements on alumina scale growth of β-NiAl at 1200 °C. Corros Sci. 2014;88:197.
[5] Li D, Guo H, Wang D, Zhang T, Gong S, Xu H. Cyclic oxidation of β-NiAl with various reactive element dopants at 1200 °C. Corros Sci. 2013;66:125.
[6] Yan K, Guo H, Gong S. High-temperature oxidation behavior of β-NiAl with various reactive element dopants in dry and humid atmospheres. Corros Sci. 2014;83:335.
[7] Dong Z, Peng X, Guan Y, Li L, Wang F. Optimization of composition and structure of electrodeposited Ni–Cr composites for increasing the oxidation resistance. Corros Sci. 2012;62:147.

[8] Young DJ, Zurek J, Singheiser L, Quadakkers WJ. Temperature dependence of oxide scale formation on high-Cr ferritic steels in Ar–H_2–H_2O. Corros Sci. 2011;53(6):2131.
[9] Yang Z, Xia GG, Stevenson JW. Evaluation of Ni–Cr-base alloys for SOFC interconnect applications. J Power Sources. 2006;160(2):1104.
[10] Caplan D, Cohen M. The volatilization of chromium oxide. J Electrochem Soc. 1961;108(5):438.
[11] Berthod P. Kinetics of high temperature oxidation and chromia volatilization for a binary Ni–Cr alloy. Oxid Met. 2005;64(3):235.
[12] Tedmon CS. The effect of oxide volatilization on the oxidation kinetics of Cr and Fe–Cr alloys. J Electrochem Soc. 1966;113(8):766.
[13] Qin L, Pei Y, Li S, Zhao X, Gong S, Xu H. Role of volatilization of molybdenum oxides during the cyclic oxidation of high-Mo containing Ni-based single crystal superalloys. Corros Sci. 2017;129:192.
[14] Goebel JA, Pettit FS, Goward GW. Mechanisms for the hot corrosion of nickel-base alloys. Metall Mater Trans. 1973;4(1):261.
[15] Carrasco JG, Adeva P, Aballe M. The role of microstructure on oxidation of Ni–Cr–Al base alloys at 1023 and 1123 K in air. Oxid Met. 1990;33(1–2):1.
[16] Hashizume R, Yoshinari A, Kiyono T, Murata Y, Morinaga M. Development of Ni-based single crystal superalloys for power-generation gas turbines. In: Proceedings of the 10th international symposium on superalloys. Pennsylvania; 2004. 483.
[17] Hobbs RA, Brewster GJ, Rae CM, Tin S. Evaluation of ruthenium-bearing single crystal superalloys—a design of experiments. In: Proceedings of the 11th international symposium on superalloys, Pennsylvania; 2008. 171.
[18] Park SJ, Seo SM, Yoo YS, Jeong HW, Jang HJ. Effects of Al and Ta on the high temperature oxidation of Ni-based superalloys. Corros Sci. 2015;90:305.
[19] Park SJ, Seo SM, Yoo YS, Jeong HW, Jang HJ. Effects of Ti on high temperature oxidation of Ni-based superalloys. Corros Sci Technol. 2016;15(3):129.
[20] Kim HS, Park SJ, Seo SM, Yoo YS, Jeong HW, Jang HJ. High temperature oxidation resistance of Ni-(5–13) Co-(10–16) Cr-(5–9) W-5Al-(1–1.5) Ti-(3–6) Ta alloys. Met Mater Int. 2016;22(5):789.
[21] Jang HJ, Yun KS, Park CJ. Analysis of the Effects of Ti, Si, and Mo on the resistance to corrosion and oxidation of Fe–18Cr stainless steels by response surface methodology. Korean J Met Mater. 2010;48(8):741.
[22] Yang DC, Jang IS, Jang MH, Park CN, Park CJ, Choi J. Optimization of additive compositions for anode in Ni-MH secondary battery using the response surface method. Met Mater Int. 2009;15(3):421.
[23] Nikrooz B, Zandrahimi M. Optimization of process variables and corrosion properties of a multi layer silica sol gel coating on AZ91D using the Box–Behnken design. J Sol–Gel Sci Technol. 2011;59(3):640.
[24] Leigh S, Sezer K, Li L, Grafton-Reed C, Cuttell M. Statistical analysis of recast formation in laser drilled acute blind holes in CMSX-4 nickel superalloy. Int J Adv Manuf Technol. 2009;43(11):1094.
[25] Kircher TA, McMordie BG, Richards K. Use of experimental designs to evaluate formation of aluminide and platinum aluminide coatings. Surf Coat Technol. 1998;108(10):24.
[26] Blaikie Norman. Analyzing Quantitative Data: From Description to Explanation. London: SAGE publications Ltd; 2003.
[27] Huang X, Li J, Hu R, Bai G, Fu H. Evolution of oxidation in Ni–Cr–W alloy at 1100 °C. Rare Met Mater Eng. 2010;39(11):1908.
[28] Sato A, Chiu YL, Reed RC. Oxidation of nickel-based single-crystal superalloys for industrial gas turbine applications. Acta Mater. 2011;59(1):225.
[29] Irving GN, Stringer J, Whittle DP. The oxidation of Co-20% Cr base alloys containing Nb or Ta. Corros Sci. 1975;15(5):337.
[30] Guo H, Wang D, Peng H, Gong S, Xu H. Effect of Sm, Gd, Yb, Sc and Nd as reactive elements on oxidation behaviour of β-NiAl at 1200 °C. Corros Sci. 2014;78:369.